AGU PUBLICATIONS

Water Resources Research

RESEARCH ARTICLE
10.1002/2014WR016096

Key Points:
- New exact solution for interface flow in confined aquifer
- Dupuit interface gives good prediction of toe position in isotropic aquifers
- Lumped resistance along streambed improves Dupuit models with anisotropy

Correspondence to:
M. Bakker,
mark.bakker@tudelft.nl

Citation:
Bakker, M. (2014), Exact versus Dupuit interface flow in anisotropic coastal aquifers, *Water Resour. Res.*, *50*, doi:10.1002/2014WR016096.

Received 3 JUL 2014
Accepted 20 SEP 2014
Accepted article online 24 SEP 2014

Exact versus Dupuit interface flow in anisotropic coastal aquifers

Mark Bakker[1]

[1]Water Resources Section, Faculty of Civil Engineering and Geosciences, Delft University of Technology, Delft, Netherlands

Abstract The Dupuit solution for interface flow toward the coast in a confined aquifer is compared to a new exact solution, which is obtained with the Hodograph method and conformal mapping. The position of the toe of the interface is a function of two dimensionless parameters: the ratio of the hydraulic gradient upstream of the interface where flow is one-dimensional over the dimensionless density difference, and the ratio of the horizontal hydraulic conductivity over the vertical hydraulic conductivity. The Dupuit interface, which neglects resistance to vertical flow, is a very accurate approximation of the exact interface for isotropic aquifers. The difference in the position of the toe between the exact and Dupuit solutions increases when the vertical anisotropy increases. For highly anistropic aquifers, it is proposed to add an effective resistance layer along the bottom of the sea in Dupuit models. The resistance of the layer is chosen such that the head in the Dupuit model is equal to the head in the exact solution upstream of the interface where flow is one-dimensional.

1. Introduction

Seawater intrusion in coastal aquifers may be simulated as interface flow when the transition zone between the freshwater and saltwater is relatively thin. A convenient approach for the simulation of interface flow is the adoption of the Dupuit approximation [e.g., *Strack*, 1976; *Cheng et al*., 2000; *Bakker*, 2003; *Pool and Carrera*, 2011]. In Dupuit interface models, the resistance to vertical flow is neglected within an aquifer, so that the vertical head distribution is hydrostatic. As a result, the spatial dimension of the problem is reduced by one. It is emphasized that the resulting flow field is still three-dimensional, as the vertical component of the flow may be computed from continuity of flow [*Strack*, 1984; *Bakker*, 1998]. Application of Dupuit interface models for the simulation of regional flow in coastal aquifers is increasing since the release of the Seawater Intrusion Package (SWI2) for MODFLOW2005 [*Bakker et al*., 2013]. The question that arises is how accurate the Dupuit interface is, especially in vertically anisotropic aquifers, and how the coastal boundary can be represented most accurately in Dupuit models such as MODFLOW/SWI.

The performance of the Dupuit approximation for interface flow is assessed in this paper by considering the problem of uniform flow toward the coast in a vertical cross section of a confined aquifer, where the sea bottom is approximated as horizontal (Figure 1). *Bear and Dagan* [1964] presented a solution to this problem for isotropic aquifers through application of the hodograph method and conformal mapping. They did not succeed in obtaining a solution in closed form. Their solution includes an integral that must be evaluated numerically and includes parameters that are difficult to evaluate for many cases, without further enhancements, using standard computer precision. *Strack* [1995] presented the solution to a much more complicated problem by including a drain in the freshwater zone. *De Josselin de Jong* [1965] solved the related problem of interface flow to a drain along the confining top of an infinitely thick aquifer; this solution reduces to the much simpler *Glover* [1959] solution when the discharge of the drain is set to zero. *Kacimov and Obnosov* [2001] presented an analytic solution for the shape of the interface for the problem of Figure 1 when the seabottom makes an arbitrary angle with the horizontal using the method of Polubarinova-Kochina.

In this paper, an exact solution to the flow problem of Figure 1, including vertical anisotropy, is obtained in closed form, using a different mapping than *Bear and Dagan* [1964], and the solution is written in a form that is amenable to numerical evaluation for a large range of realistic parameters. Furthermore, it is shown that the position of the toe of the interface is a function of only two dimensionless parameters. The exact

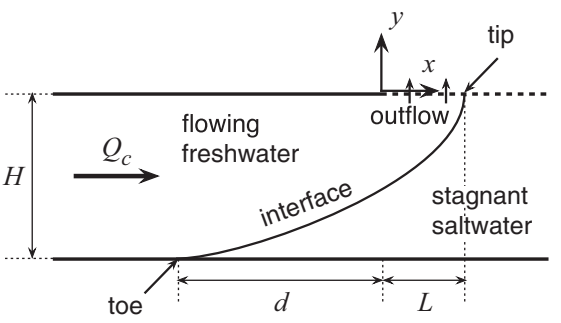

Figure 1. Interface flow in a vertical cross section of a confined aquifer.

solution is used to assess the accuracy of the Dupuit solution. Finally, a coastal boundary condition for Dupuit interface models is proposed to improve results for vertically anisotropic aquifers.

2. Problem Description

Consider steady interface flow in a vertical cross section of a horizontal confined aquifer of thickness H (Figure 1); the saltwater is stagnant. A Cartesian x, y coordinate system is adopted with its origin at the coastline; the y axis points vertically upward (z is used for complex coordinates). The aquifer extends to infinity to the left and right. The principal directions of the hydraulic conductivity tensor are horizontal and vertical, and the corresponding principal components are k_x and k_y, respectively. The top and bottom of the confined aquifer are impermeable except below the sea, where the seabottom is represented by a horizontal constant-head boundary. The vertical datum is chosen such that the equivalent freshwater head along the sea bottom is zero. In the left part of the aquifer, the freshwater flow is confined, and the groundwater discharge toward the coast is equal to Q_c [L^2/T]

$$Q_c = k_x H g_c \tag{1}$$

where g_c equals the absolute value of the head gradient upstream in the confined part of the aquifer, where flow is one-dimensional; for brevity, g_c will simply be referred to as "the upstream gradient" in this paper. The dimensionless density difference ν_s is defined as

$$\nu_s = (\rho_s - \rho_f)/\rho_f \tag{2}$$

where ρ_s is the density of saltwater and ρ_f is the density of freshwater. The distance between the toe of the interface and the coastline is called d and the length of the outflow zone along the bottom of the sea is called L. The tip of the interface is the point where the interface intersects the sea bottom.

The components of the specific discharge vector in the freshwater zone may be written as

$$q_x = -k_x \frac{\partial h}{\partial x} \qquad q_y = -k_y \frac{\partial h}{\partial y} \tag{3}$$

where h is the freshwater head defined as [e.g., *Post et al.*, 2007]

$$h = \frac{p}{\rho_f g} + y \tag{4}$$

where p is the pressure and g is the acceleration of gravity. Application of continuity of flow gives the following differential equation for the head in the freshwater zone

$$\frac{\partial}{\partial x}\left(k_x \frac{\partial h}{\partial x}\right) + \frac{\partial}{\partial y}\left(k_y \frac{\partial h}{\partial y}\right) = 0 \tag{5}$$

A scaled ξ, η coordinate system is used to transform the differential equation to Laplace's equation [e.g., *Bear and Dagan*, 1965]

$$\frac{\partial^2 h}{\partial \xi^2} + \frac{\partial^2 h}{\partial \eta^2} = 0 \tag{6}$$

where

$$\xi = x/\sqrt{\alpha} \qquad \eta = y \tag{7}$$

where α is the anisotropy ratio defined as

$$\alpha = k_x/k_y \tag{8}$$

The components of the specific discharge vector in the scaled domain are

$$q_\xi = -k\frac{\partial h}{\partial \xi} \qquad q_\eta = -k\frac{\partial h}{\partial \eta} \tag{9}$$

where the isotropic hydraulic conductivity k in the scaled domain equals

$$k = \sqrt{k_x k_y} \tag{10}$$

The flow in the scaled domain is related to the flow in the physical domain as

$$q_x = q_\xi \qquad q_y = q_\eta/\sqrt{\alpha} \tag{11}$$

As flow in the scaled domain is governed by Laplace's equation, the problem may be written in terms of a complex potential Ω [e.g., *Strack*, 1989]

$$\Omega = \Phi + i\Psi \tag{12}$$

where

$$\Phi = kh \tag{13}$$

is the specific discharge potential and Ψ is the stream function. The components of the specific discharge vector in the scaled domain are related to the specific discharge potential as

$$q_\xi = -\frac{\partial \Phi}{\partial \xi} \qquad q_\eta = -\frac{\partial \Phi}{\partial \eta} \tag{14}$$

and the complex specific discharge function W is defined as

$$W = q_\xi - iq_\eta = -\frac{\mathrm{d}\Omega}{\mathrm{d}z} \tag{15}$$

where $z = \xi + i\eta$ is the complex coordinate in the scaled domain. In the scaled domain, the specific discharge potential Φ equals zero along the seabed (the outflow zone). The stream function is chosen to be zero along the impermeable top boundary of the aquifer and equals Q_c along the bottom of the aquifer and the interface.

3. Exact Solution

An exact solution to the problem of Figure 1 is obtained with the Hodograph method [e.g., *Bear and Dagan*, 1964; *Verruijt*, 1970; *Bear*, 1972; *Strack*, 1989]. Boundary segments are labeled as follows (Figure 2a). Segment $A - B$ is the interface. Segment $B - C$ is the outflow zone. Segment $C - D$ is the impermeable upper boundary of the confined aquifer, where point D lies at $\xi = -\infty$. Segment $D - A$ is the impermeable bottom boundary of the aquifer. The boundary of the scaled flow domain in the complex potential plane is shown in Figure 2b. The boundary of the scaled flow domain in the W plane is shown in Figure 2c while the inverse of the W plane, the W^{-1} plane, is shown in Figure 2d. The boundary in the W^{-1} domain consists of straight line segments, which is much easier to deal with than a boundary consisting of straight line segments and circular arcs [e.g., *Bakker*, 2000].

Both the Ω and W^{-1} planes are mapped onto an auxiliary complex t plane. The real parts of both Ω and W are constant and equal to zero along $B - C$, while the imaginary parts are piecewise constant along the other segments. This makes it promising to choose the t plane as the quarter plane shown in Figure 2e, where point B is at infinity and point C is at the origin so that segment $B - C$ lies along the positive imaginary axis and the other segments along the positive real axis. The only other point that is fixed in the mapping is point A, which is put at $t = 1$. The location of point D is dictated by the mapping and lies along the real axis at $t = \tau$ between points C and A. Note that, even without solving the problem, it may be concluded that the outflow along the seabed varies from $q_\eta = kv_s$ (i.e., $q_y = k_y v_s$) at point B to infinity at point C [see, e.g., *Strack*, 1989, Example 46.1].

Details of the solution are given in Appendix A, where special care is taken to write the equations in forms that are suitable for evaluation on a computer. The solution is obtained in parametric form as $x(t)$, $y(t)$, and $\Omega(t)$:

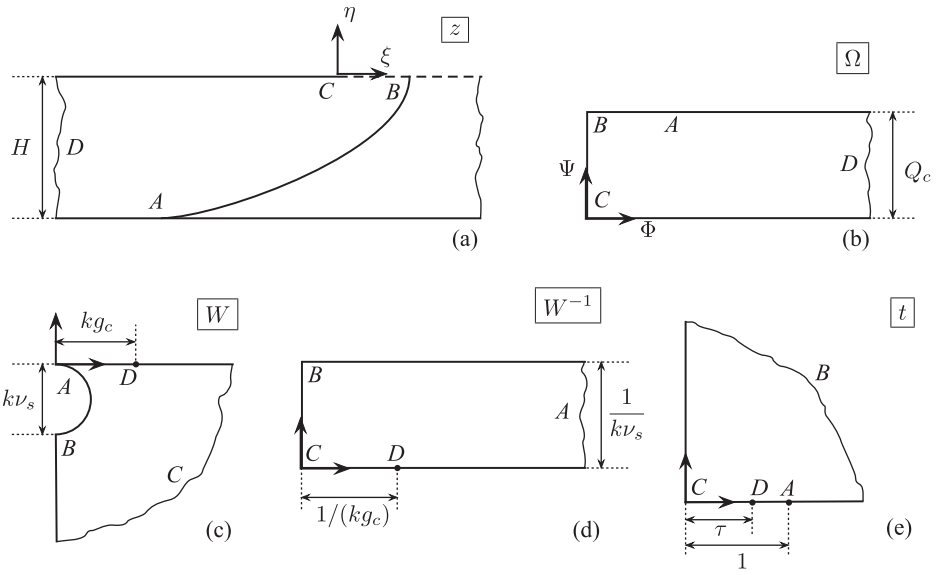

Figure 2. (a) Scaled domain, (b) Ω plane, (c) *W* plane, (d) W^{-1} plane, and (e) *t* plane.

$$\frac{x}{H} = \frac{-g_c\alpha}{\pi^2 v_s}\Re[\mathsf{F}(t)-\mathsf{F}(0)]$$
$$\frac{y}{H} = \frac{-g_c\sqrt{\alpha}}{\pi^2 v_s}\Im[\mathsf{F}(t)-\mathsf{F}(0)] \tag{16}$$

$$\frac{\Omega}{kHv_s} = \frac{h}{v_s H} + \frac{\Psi}{kHv_s}i = -\frac{g_c\sqrt{\alpha}}{v_s\pi}\left[\ln\left(\frac{t-\tau}{t+\tau}\right)+i\right] \tag{17}$$

where $\mathsf{F}(t)$ is given by (A11) and τ is given by (A4). Note that both the normalized *x*, *y* location and the normalized head and stream function are fully determined by only two dimensionless parameters: the ratio of the upstream gradient g_c over the dimensionless density v_s, and the anisotropy ratio $\alpha = k_x/k_y$. The easiest way to evaluate the solution is by specifying the head and stream function of the point of interest, compute the corresponding value of *t* with the inverse of (17) and then use that *t* value to compute the *x*, *y* location with (16). Details are given at the end of the Appendix A.

4. Dupuit Solution

The Dupuit solution is obtained with the *Strack* potential [*Strack*, 1976]. In the standard application of the Dupuit approximation, the head along the coastline is set equal to sea level (zero in this case) and the interface is at the top of the aquifer. The solution is straightforward and is presented here without further derivation. The Strack potential Φ_s for uniform flow toward the coast is

$$\Phi_s = -Q_c x \tag{18}$$

where the relationship between the potential and the head is

$$\Phi_s = \frac{1}{2}k_x h_d^2/v_s \qquad h_d \le v_s H$$
$$\Phi_s = k_x H h_d - \frac{1}{2}k_x v_s H^2 \qquad h_d \ge v_s H \tag{19}$$

where h_d is the head in the Dupuit solution. The distance between the toe and the coastline in the Dupuit solution is called d_d. At the toe, $x = -d_d$ and $h_d = v_s H$, which means the potential equals $\Phi_s = \frac{1}{2}k_x v_s H^2$, so that

$$\frac{d_d}{H} = \frac{v_s}{2g_c} \tag{20}$$

Note that in regular confined flow (no interface flow), $h_d = v_s H$ is reached when $d_d/H = v_s/g_c$, which is exactly twice as large as for confined interface flow. The vertical elevation of the interface ζ is obtained from the head with the Ghyben-Herzberg relation

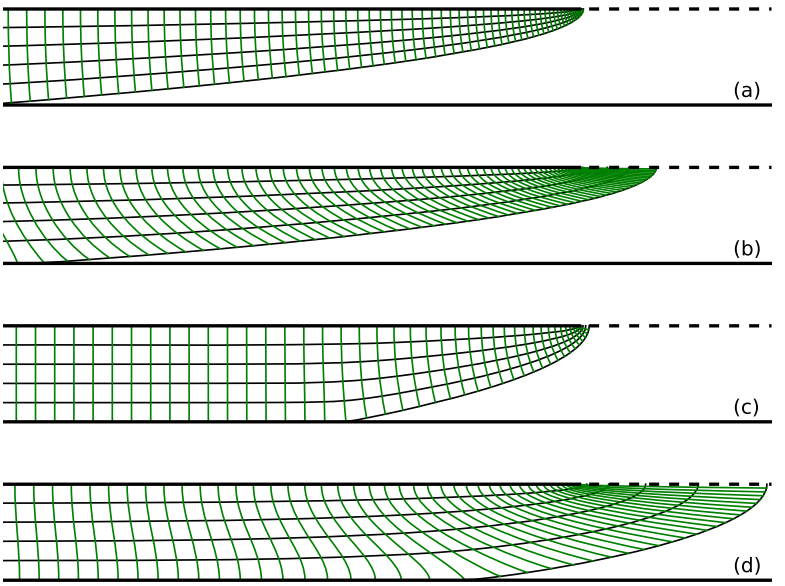

Figure 3. Flow nets for (a) g_c/v_s=0.08 and $\alpha = 1$, (b) g_c/v_s=0.08 and $\alpha = 20$, (c) g_c/v_s=0.2 and $\alpha = 1$, and (d) g_c/v_s=0.2 and $\alpha = 20$. Horizontal and vertical scales are equal.

$$\zeta = -h_d/v_s \qquad h_d \leq v_s H \tag{21}$$

5. Comparison of the Exact and Dupuit Solutions

Flow nets are computed for two anisotropy ratios $\alpha = 1$ (isotropic) and $\alpha = 20$ and for two upstream gradients: g_c=0.002 and g_c=0.005; the dimensionless density is v_s=0.025 for all cases, as is reasonable for seawater [e.g., *Post et al.*, 2007]. The flow nets are shown in Figure 3. The position of the toe of the interface moves to the coast and the length of the outflow zone increases when the term g_c/v_s increases and/or the anisotropy ratio increases. Note that the interface is horizontal at the toe ($W = 0$, Figure 2c), but the interface curves up quickly so that this is not visible in the figures. The larger value of g_c is larger than the gradient in most coastal aquifers, but the solution is valid for any combination of g_c/v_s=0.2, for example a much more realistic gradient of g_c=0.001 and an aquifer filled with brackish water with v_s=0.005.

For the same four cases, the exact interface is compared to the Dupuit interface (Figure 4). The length of the outflow zone is zero in the Dupuit solution for all cases. The exact interface (black for $\alpha = 1$ and blue for $\alpha = 20$) is always deeper than the Dupuit interface (red), and the toe of the Dupuit interface is always farther inland (i.e., conservative). The Dupuit interface is a very good approximation of the two isotropic cases. When $\alpha = 20$, it is still a reasonable approximation when g_c/v_s=0.08, but less so when g_c/v_s=0.2.

A graph is created of the distance d between the toe of the interface and the coastline as a function of g_c/v_s for two different anisotropy ratios (Figure 5a). The toe according to the Dupuit solution is shown with red dots (dots are used rather than a line, else the Dupuit and exact isotropic case virtually overlap). The Dupuit solution is a very good approximation of the toe of the exact solution for the isotropic case (black line) and is a good but conservative estimate for the cases with an anisotropy ratio of 20. The difference in toe location between the Dupuit solution and the exact solution is shown in Figure 5b and is less than 10 percent of the aquifer thickness for the isotropic case for all values of g_c/v_s. For a high anisotropy ratio of 20, the difference is less than half an aquifer thickness when $g_c/v_s < 0.075$ and less than one aquifer thickness when $g_c/v_s < 0.15$. Note that the latter value of g_c/v_s corresponds to a large gradient of g_c=0.00375 when the aquifer is filled with seawater (v_s=0.025), but a much smaller g_c=0.0015 for brackish aquifers with 40 percent seawater (v_s=0.01).

The heads of the exact solution and the Dupuit solution are compared for the case that g_c/v_s=0.2 in Figure 6 (this is the case of Figure 3d). Heads are plotted along the top of the aquifer (solid lines) and along the bottom of the aquifer and interface (dashed lines) for the isotropic case (black lines) and the case with

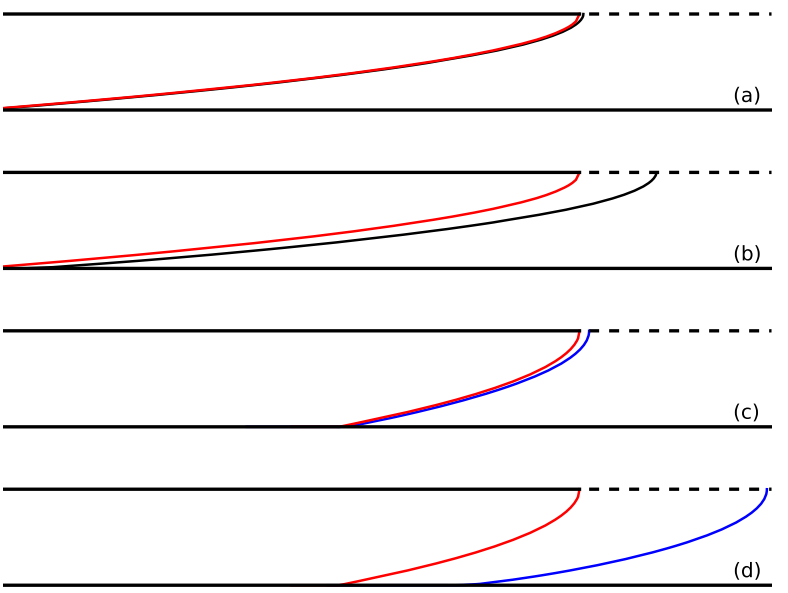

Figure 4. Exact interface (black is $\alpha = 1$ and blue is $\alpha = 20$) and Dupuit interface (red) for (a) g_c/v_s=0.08 and $\alpha = 1$, (b) g_c/v_s=0.08 and $\alpha = 20$, (c) g_c/v_s=0.2 and $\alpha = 1$, (d) g_c/v_s=0.2 and $\alpha = 20$. Horizontal and vertical scales are equal.

$\alpha = 20$ (blue lines). The head along the bottom/interface is always larger than at the top of the aquifer, as expected. The red dots in the graph indicate the head in the Dupuit solution, which is very close to the head at the top of the aquifer for the isotropic case. The green dots represent a Dupuit solution with a different coastal boundary condition, which will be explained in the next section. The horizontal dotted line indicates the head along the interface corresponding to the toe. Upstream of the toe, the head at the top and bottom of the aquifer converge to the same line with a gradient of minus g_c. There is a consistent difference of approximately $0.12 v_s H$ between the Dupuit head (red dots) and the exact head for this case with $\alpha = 20$ (blue lines).

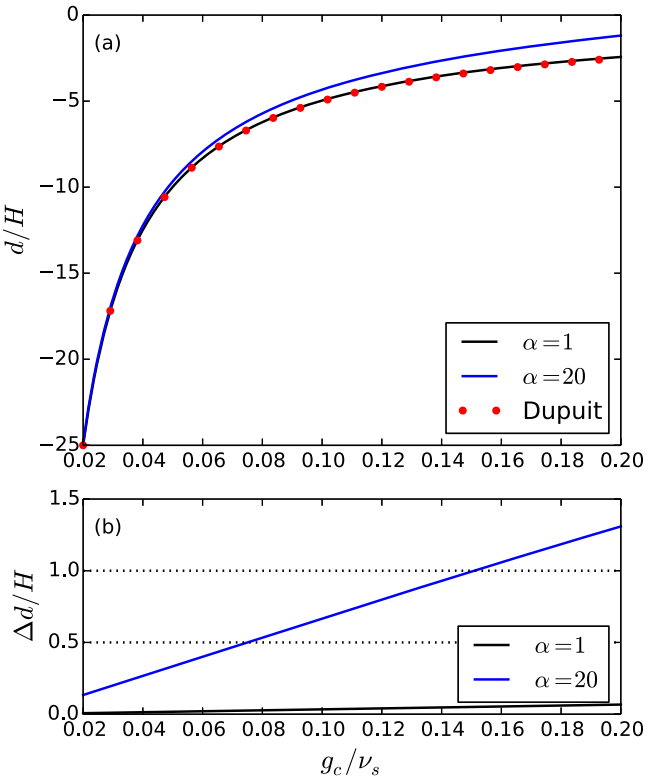

Figure 5. (a) Distance d between interface toe and coastline versus upstream gradient g_c divided by dimensionless density difference v_s for two anisotropy ratios α and the Dupuit solution. (b) Difference between d for exact and Dupuit solutions.

6. Dupuit Model With Effective Resistance Layer Along Seabed

As the resistance to vertical flow is neglected in a Dupuit model, the length of the outflow zone is zero and the thickness of the freshwater zone is smaller everywhere as compared to the exact solution. Although this means that the Dupuit solution is conservative, it also results in a consistent error in head (Figure 6). This error is negligibly small for isotropic aquifers, but can become significant when both the term g_c/v_s and the anisotropy

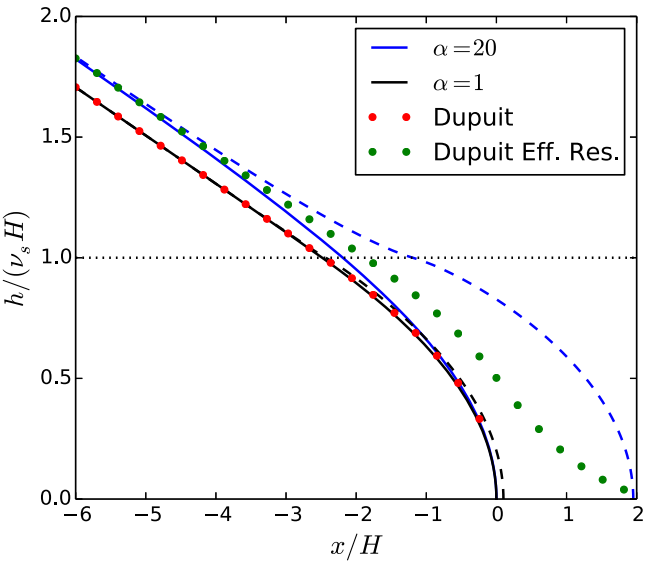

Figure 6. Head along the top of the aquifer (solid lines) and bottom of the aquifer or interface (dashed lines) for the exact solution for the case that $g_c/\nu_s = 0.2$. Red dots represent Dupuit solution. Green dots represent Dupuit solution for $\alpha = 20$ with effective resistance layer along seabed.

ratio are large. This is undesirable, as the error in head affects the entire model. If the upstream boundary condition is head-specified rather than flux specified, the Dupuit model will underestimate the flow toward the coast.

It is proposed to change the boundary condition along the coast in Dupuit models by lumping the vertical resistance of the aquifer in an effective resistance layer along the bottom of the sea, as shown in Figure 7. The vertical component of the specific discharge vector q_y through the resistance layer (the outflow) is computed as

$$q_y = (h_d - h_s)/c \tag{22}$$

where h_s is the head in the sea (set to zero in this paper), and c is the effective resistance of the resistance layer (to be determined later). The approach of adding an effective resistance layer is inspired by the work of *Anderson* [2003, 2005], who added an effective resistance layer to the bottom of a lake to simulate accurately the interaction between groundwater and surface water with a Dupuit model.

A Dupuit solution for the problem shown in Figure 7 was presented by *Bakker* [2006]. For the case that the toe of the interface is upstream of the coastline and the resistance layer is longer than the outflow zone, the solution is (written in terms of the variables used in this paper):

$$\begin{aligned}
\frac{h_d}{\nu_s H} &= \frac{H}{6 k_x c}\left(\frac{x}{H} - \frac{L_d}{H}\right)^2 \qquad 0 \le x \le L_d \\
\frac{h_d}{\nu_s H} &= \sqrt{1 - 2\frac{g_c}{\nu_s}\left(\frac{x}{H} + \frac{d_d}{H}\right)} \qquad -d_d \le x \le 0 \\
\frac{h_d}{\nu_s H} &= \frac{-g_c}{\nu_s}\left(\frac{x}{H} + \frac{d_d}{H}\right) + 1 \qquad x \le -d_d
\end{aligned} \tag{23}$$

where L_d is the length of the outflow zone in the Dupuit solution with an effective resistance layer

$$\frac{L_d}{H} = \left(\frac{18 g_c}{\nu_s}\right)^{1/3}\left(\frac{k_x c}{H}\right)^{2/3} \tag{24}$$

and d_d is the distance between the toe and the coast line in the Dupuit solution with an effective resistance layer

$$\frac{d_d}{H} = \frac{\nu_s}{2 g_c}\left[1 - \left(\frac{3}{2}\frac{g_c^2}{\nu_s^2}\frac{k_x c}{H}\right)^{2/3}\right] \tag{25}$$

Note that d_d/H equals $\nu_s/(2g_c)$ (equation (20)) when c equals zero.

The effective resistance c is computed such that that the head obtained from the exact solution is the same as the head computed with the Dupuit solution upstream of the toe, where the flow is one-dimensional. The two heads are set equal at the location $x = x^*$ where the head h of the exact solution is twice the head at the toe

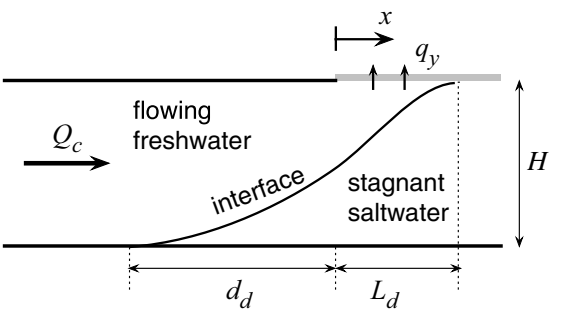

Figure 7. Proposed boundary condition along seabed in Dupuit models. The effective resistance c of the resistance layer (gray) represents the resistance to vertical flow.

$$h(x^*, 0) = 2v_s H \tag{26}$$

The Dupuit head h_d (last equation of (23)) is set equal to $2v_s H$ at $x = x^*$

$$\frac{-g_c}{v_s}\left(\frac{x^*}{H} + \frac{d_d}{H}\right) + 1 = 2 \tag{27}$$

Substitution of (25) for d_d and some algebra gives a formula for the effective resistance c normalized through division by the vertical resistance of the aquifer H/k_y

$$\frac{ck_y}{H} = \frac{2v_s^2}{3g_c^2\alpha}\left(3 + \frac{2g_c x^*}{v_s H}\right)^{3/2} \tag{28}$$

The value of x^* may be computed by first computing the value of t with (A13) using $\hat{\Omega} = 2v_s kH$, then computing z with (A12) and finally x^* is obtained from the inverse of (7). As an example, the head is computed for the case of Figure 3d. Use of an effective resistance layer results in no upstream head difference between the exact solution and the Dupuit solution, as shown with the green dots in Figure 6.

The normalized effective resistance is a function of the ratio g_c/v_s and of the anisotropy ratio and is plotted in Figure 8. The flux toward the coast likely varies along the coastline in a three-dimensional model of a coastal aquifer. As the effective resistance is a function of the flux, it may be necessary to select an average value for the range of fluxes that may be expected. It is emphasized that the addition of the resistance layer to the model, as shown in Figure 7, is only needed when the anisotropy factor is high.

Addition of the effective resistance layer along the seabottom negates any error in the head upstream of the toe where flow is one-dimensional. It also improves the position of the toe and it adds an outflow zone to the Dupuit solution. The length of the outflow zone is similar to the length of the outflow zone of the exact solution (Figure 9), but the shape is different. At the tip of the interface, the upward flux is $q_y = k_y v_s$ in the exact solution, as stated earlier, and the horizontal flux is zero, so that the interface is vertical. In the Dupuit solution with the effective resistance layer, the flux is zero at the tip, and hence the interface is horizontal.

7. Conclusions and Discussion

A new closed-form exact solution is presented for interface flow in confined coastal aquifers with an anisotropic hydraulic conductivity. The sea bottom is approximated with a horizontal constant-head boundary. The dimensionless location of the toe of the interface is a function of just two dimensionless parameters: the ratio of the upstream gradient g_c over the dimensionless density difference v_s, and the anisotropy ratio $\alpha = k_x/k_y$. The existing Dupuit solution to the same problem is written in terms of the Strack potential where the interface is set to the top of the aquifer at the coastline. The Dupuit solution is a very accurate approximation of the exact solution for isotropic aquifers. For anisotropic aquifers, the difference between the interface toe of the exact and Dupuit solutions increases but the difference remains less than $1.5H$ when $g_c/v_s < 0.2$ (Figure 5).

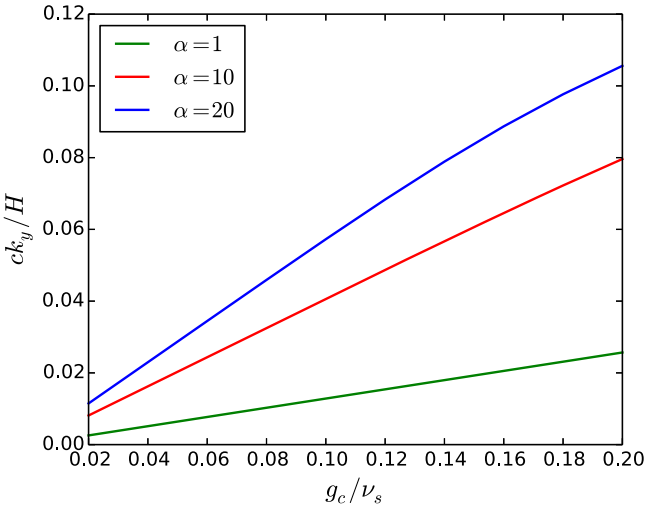

Figure 8. Vertical resistance c of effective resistance layer as a factor times the vertical resistance of the aquifer (H/k_y).

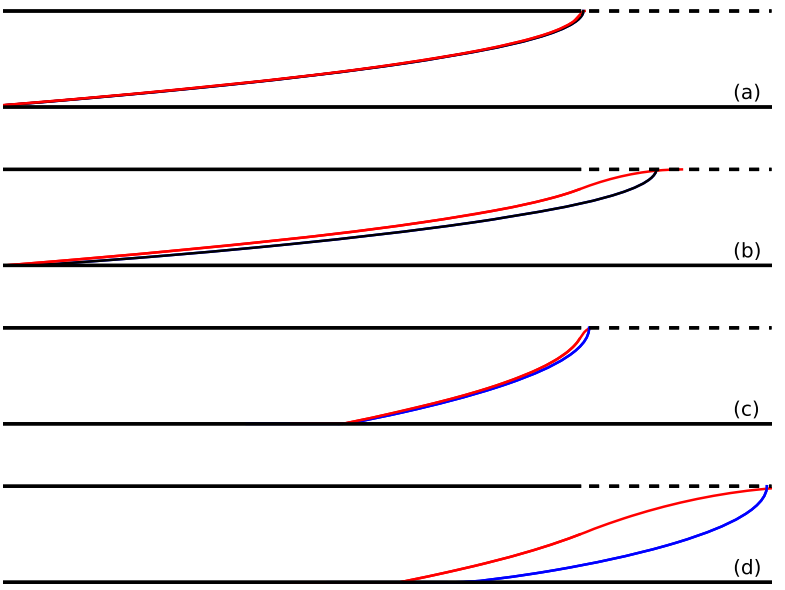

Figure 9. Exact interface (black is $\alpha = 1$ and blue is $\alpha = 20$) and Dupuit interface with effective resistance layer (red) for (a) g_c/v_s=0.08 and $\alpha = 1$, (b) g_c/v_s=0.08 and $\alpha = 20$, (c) g_c/v_s=0.2 and $\alpha = 1$, (d) g_c/v_s=0.2 and $\alpha = 20$. Horizontal and vertical scales are equal.

Bear and Dagan [1964] concluded that the Ghyben-Herzberg relationship (and thus a Dupuit model) is a good approximation for isotropic aquifers when $\pi k v_s H/Q_c > 8$, which translates to $g_c/v_s < \pi/8 \approx 0.39$. This value is equivalent to $g_c \approx 0.01$ when v_s=0.025, corresponding to a toe location of $d \approx H$, which means seawater intrusion is almost negligible. So in practice, the conclusion is the same as the one reached in this paper: a Dupuit interface is very accurate for isotropic aquifers filled with seawater.

A new coastal boundary condition is proposed so that Dupuit interface models of anisotropic aquifers do not result in a consistent error in the head upstream of the interface where flow becomes one-dimensional. Application of the new coastal boundary for Dupuit interface models results in an outflow zone along the sea bottom, which is required in, for example, the SWI2 package for MODFLOW [*Bakker et al.*, 2013]. The new boundary condition lumps the resistance to vertical flow into an effective resistance layer at the bottom of the sea. The resistance c of this effective resistance layer is a function of the ratio g_c/v_s and of the anisotropy ratio α (Figure 8). The effective resistance depends on the flow, which may vary along the coast in regional Dupuit models of seawater intrusion, especially when vertical pumping wells are located near the coast. Vertical wells are commonly located as far as possible from the coast to reduce the possibility of seawater intrusion, so that the flow at the coastline is predominantly normal to the coastline. For such cases, a practical solution is to use an average value for c based on the range of flow values that may be expected in the model. Further research is needed to assess the accuracy of the proposed effective resistance in regional models with vertical wells pumping along the coast.

Appendix A: Derivation of the Exact Solution

The exact solution to the problem shown in Figure 2 is derived following the approach outlined in *Strack* [1989]. The boundaries of the domains in the Ω and W^{-1} planes (Figures 2b and 2d) have the same shape. They are purely imaginary along B – C, and their imaginary parts are piecewise constant along the other segments. Ψ jumps from 0 to Q_c at $t=\tau$ and $\Im W^{-1}$ jumps from 0 to $1/(kv_s)$ at $t = 1$. The conformal mapping of these domains onto the t plane may be obtained using image wells as [e.g., *Anderson*, 2005]

$$\Omega = \frac{-Q_c}{\pi} \ln\left(\frac{t-\tau}{t+\tau}\right) + Q_c i \tag{A1}$$

$$\frac{1}{W} = \frac{-1}{\pi k v_s} \ln\left(\frac{1-t}{1+t}\right) \tag{A2}$$

The value of τ can be obtained by requiring that $W^{-1}=H/Q_c$ at $t=\tau$, which gives

$$\ln\left(\frac{1-\tau}{1+\tau}\right)=\frac{-\pi v_s}{g_c\sqrt{\alpha}}=a \tag{A3}$$

where the new variable a is introduced for convenience and it is used that $Q_c=k_xHg_c$. An expression for τ may be obtained from (A3) after some algebra as

$$\tau=1+\varepsilon \tag{A4}$$

where

$$\varepsilon=\frac{-2e^a}{1+e^a} \tag{A5}$$

which can be evaluated accurately for very small values of a.

An expression for z is obtained from [e.g. *Strack*, 1989]

$$z=\int -\frac{1}{W}\frac{\mathrm{d}\Omega}{\mathrm{d}t}\mathrm{d}t \tag{A6}$$

Substitution of the derivative of (A1) for $\mathrm{d}\Omega/\mathrm{d}t$ and (A2) for W^{-1} in (A6) and combining terms gives

$$z=\frac{-Q_c}{\pi^2 k v_s}\mathrm{F}(t) \tag{A7}$$

where

$$\mathrm{F}(t)=\int\left[\frac{\ln(1-t)}{t-\tau}-\frac{\ln(1-t)}{t+\tau}-\frac{\ln(1+t)}{t-\tau}+\frac{\ln(1+t)}{t+\tau}\right]\mathrm{d}t \tag{A8}$$

All four terms in the integrand of (A8) turn into a combination of logarithms and dilogarithms, the latter being defined as [e.g., *Strack*, 1989, Appendix B]

$$\mathrm{Li}_2(t)=-\int_0^t\frac{\ln(1-s)}{s}ds \tag{A9}$$

All terms in the integrand of (A8) have the same form and may be integrated as

$$\int_0^t\frac{\ln(1\pm s)}{s+b}\mathrm{d}s=\int_0^t\frac{\ln\left[(1+b)\left(1-\frac{s+b}{1+b}\right)\right]}{s+b}\mathrm{d}s=\ln(1\mp b)\ln(t+b)-\mathrm{Li}_2\left(\frac{t+b}{\mp 1+b}\right) \tag{A10}$$

where b is an arbitrary constant. Integration of (A8) now gives

$$\begin{aligned}\mathrm{F}=\;&\ln(1-\tau)\ln(t-\tau)-\ln(1+\tau)\ln(t+\tau)-\ln(1+\tau)\ln(t-\tau)+\ln(1-\tau)\ln(t+\tau)\\&-\mathrm{Li}_2\left(\frac{t-\tau}{1-\tau}\right)+\mathrm{Li}_2\left(\frac{t+\tau}{1+\tau}\right)+\mathrm{Li}_2\left(\frac{t-\tau}{-1-\tau}\right)-\mathrm{Li}_2\left(\frac{t+\tau}{-1+\tau}\right)\end{aligned} \tag{A11}$$

The solution for the complex coordinate $z(t)$ in the scaled domain may now be written as

$$\frac{z}{H}=\frac{-g_c\alpha}{\pi^2 v_s}[\mathrm{F}(t)-\mathrm{F}(0)] \tag{A12}$$

where (1) is substituted for Q_c and (10) for k.

The easiest way to evaluate the solution is to specify the value of Ω of interest, compute the corresponding value of t with the inverse of (A1), and use that value of t to compute z with (A12). For example, if $\hat{\Omega}$ is the value of interest, the value of t may be computed from (A1) as

$$t=\left(1-\frac{2e^c}{1+e^c}\right)\tau \tag{A13}$$

where

$$c=-\pi\hat{\Omega}/Q_c+\pi i \tag{A14}$$

Computation of z requires evaluation of the dilogarithms in the function F (A11), which may be evaluated, for example, with the equations given in Appendix B of *Strack* [1989].

The presented solution suffers from a problem that is known as the crowding effect in conformal mapping. As stated, the location of point D is at $t=\tau=1+\varepsilon$ and is dictated by the mapping. As it turns out, ε is very small and τ is very close to 1 for smaller values of g_c/v_s. For example, for the case $g_c/v_s=0.08$ (Figure 3), $\varepsilon \approx 1 \cdot 10^{-17}$. This makes it difficult to evaluate $\ln(1-\tau)$, or $(t-\tau)$ when t is close to 1, using standard computer precision. The function F may be evaluated for values of τ very close to 1 when three terms are modified. First, the terms $(1-\tau)$ must be replaced by $-\varepsilon$. Second, the term $\ln(t-\tau)$ may be written as

$$\ln(t-\tau)=\ln\left(\frac{t-\tau}{t+\tau}\right)+\ln(t+\tau) \tag{A15}$$

where an accurate value of the first logarithm to the right of the equal sign may be obtained directly from (A1) when the desired value of Ω is specified. And third, the terms $t-\tau$ in the arguments of the dilogarithms can be obtained directly from (A13) as

$$t-\tau=\frac{-2e^c}{1+e^c}\tau \tag{A16}$$

Acknowledgment
Python scripts used to create Figures 3, 4, 5, 6, 8, and 9, including all data, are available from the author.

References

Anderson, E. I. (2003), The effective resistance to vertical flow in Dupuit models, *Adv. Water Resour.*, *26*, 513–523.
Anderson, E. I. (2005), Modeling groundwater-surface water interactions using the Dupuit approximation, *Adv. Water Resour.*, *28*, 315–327.
Bakker, M. (1998), Transient Dupuit interface flow with partially penetrating features, *Water Resour. Res.*, *34*, 2911–2918.
Bakker, M. (2000), The size of the freshwater zone below an elongated island with infiltration, *Water Resour. Res.*, *36*, 109–117.
Bakker, M. (2003), A Dupuit formulation for modeling seawater intrusion in regional aquifer systems, *Water Resour. Res.*, *39*, 1131, doi: 10.1029/2002WR001710.
Bakker, M. (2006), Analytic solutions for interface flow in combined confined and semi-confined, coastal aquifers, *Adv. Water Resour.*, *29*, 417–425.
Bakker, M., F. Schaars, J. D. Hughes, C. D. Langevin, and A. M. Dausman (2013), Documentation of the seawater intrusion (SWI2) package for MODFLOW, in *U. S. Geol. Surv. Tech. Meth. Ser.*, book 6, chap. A46, 47 p., U. S. Geol. Surv., Reston, Va. [Available at http://pubs.usgs.gov/tm/6a46/.]
Bear, J. (1972), *Dynamics of Flow in Porous Media*, Dover, N. Y.
Bear, J., and G. Dagan (1964), Some exact solutions of interface problems by means of the hodograph method, *J. Geophys. Res.*, *69*, 1563–1572.
Bear, J., and G. Dagan (1965), The relationship between solutions of flow problems in isotropic and anisotropic soils, *J. Hydrol.*, *3*, 88–96.
Cheng, A. D., D. Halhal, A. Naji, and D. Ouazar (2000), Pumping optimization in saltwater-intruded coastal aquifers, *Water Resour. Res.*, *36*, 2155–2165.
De Josselin de Jong, G. (1965), A many-valued hodograph in an interface problem, *Water Resour. Res.*, *1*, 543–555.
Glover, R. E. (1959), The pattern of fresh-water flow in a coastal aquifer, *J. Geophys. Res.*, *64*, 457–459.
Kacimov, A. R., and Y. V. Obnosov (2001), Analytical solution for a sharp interface problem in sea water intrusion into a coastal aquifer. Proceedings of the Royal Society of London. Series A: Mathematical, *Physical and Engineering Sciences*, *457*, 3023–3038.
Pool, M., and J. Carrera (2011), A correction factor to account for mixing in Ghyben-Herzberg and critical pumping rate approximations of seawater intrusion in coastal aquifers, *Water Resour. Res.*, *47*, W05506, doi:10.1029/2010WR010256.
Post, V., H. Kooi H, and C. Simmons (2007), Using hydraulic head measurements in variable-density ground water flow analyses, *Ground Water*, *45*, 664–671.
Strack, O. D. L. (1976), A single-potential solution for regional interface problems in coastal aquifers, *Water Resour. Res.*, *12*, 1165–1174.
Strack, O. D. L. (1984), Three-dimensional streamlines in Dupuit-Forchheimer models. *Water Resour. Res.*, *20*, 812–822.
Strack, O. D. L. (1989), *Groundwater Mechanics*, Prentice Hall, Englewood Cliffs, N. J.
Strack, O. D. L. (1995), Application of drains to interface flow in coastal aquifers, paper presented at the Symposium for G. de Josselin de Jong, Delft Univ. of Technol., Delft, Netherlands, April 1995.
Verruijt, A. (1970), *Theory of Groundwater Flow*, Macmillan, N. Y.